Journal of Biomaterials Science, Polymer Edition
Publication details, including instructions for authors and subscription information:
http://www.tandfonline.com/loi/tbsp20

Doxorubicin-Loaded Nanosized Micelles of a Star-Shaped Poly(ε-Caprolactone)-Polyphosphoester Block Co-polymer for Treatment of Human Breast Cancer

Nguyen-Van Cuong [a] , Ming-Fa Hsieh [b] , Yung-Tsung Chen [c] & Ian Liau [d]

[a] Department of Biomedical Engineering and R&D Center for Biomedical Microdevice Technology, Chung Yuan Christian University, 200 Chung Pei Road, Chung Li, Taiwan 32023

[b] Department of Biomedical Engineering and R&D Center for Biomedical Microdevice Technology, Chung Yuan Christian University, 200 Chung Pei Road, Chung Li, Taiwan 32023

[c] Department of Biomedical Engineering and R&D Center for Biomedical Microdevice Technology, Chung Yuan Christian University, 200 Chung Pei Road, Chung Li, Taiwan 32023

[d] Department of Applied Chemistry and Institute of Molecular Science, National Chiao Tung University, Hsinchu 300, Taiwan

Published online: 02 Apr 2012.

VSP

Journal of Biomaterials Science 22 (2011) 1409–1426

Journal of BIOMATERIALS SCIENCE
brill.nl/jbs

Doxorubicin-Loaded Nanosized Micelles of a Star-Shaped Poly(ε-Caprolactone)-Polyphosphoester Block Co-polymer for Treatment of Human Breast Cancer

Nguyen-Van Cuong [a], **Ming-Fa Hsieh** [a,*], **Yung-Tsung Chen** [a] **and Ian Liau** [b]

[a] Department of Biomedical Engineering and R&D Center for Biomedical Microdevice Technology, Chung Yuan Christian University, 200 Chung Pei Road, Chung Li, Taiwan 32023

[b] Department of Applied Chemistry and Institute of Molecular Science, National Chiao Tung University, Hsinchu 300, Taiwan

Received 7 December 2009; accepted 8 May 2010

Abstract

Star-shaped co-polymers based on the backbone of poly(ε-caprolactone) were synthesized by a ring-opening reaction using pentaerythritol as initiator and $Sn(Oct)_2$ as catalyst. The star-shaped poly(ε-caprolactone) polymer was then chain extended with a terminal block of poly(ethyl ethylene phosphate) to form a co-polymer, poly(ε-caprolactone)-poly(ethyl ethylene phosphate), when using the cyclic ethyl ethylene phosphate monomer. The amphiphilic block co-polymers can self-assemble into nanoscopic micelles with a mean diameter of 150 nm and a spherical shape. Additionally, the prepared micelles did not induce hemolysis and nitric oxide production *in vitro* based on nitric oxide, hemolytic tests and MTT assays. The hydrophobic micellar cores encapsulated doxorubicin (DOX) in an aqueous solution with a loading efficiency of 55.2%. The *in vitro* release of DOX from DOX-loaded micelles was pH dependent. DOX-loaded micelles present significantly enhanced cytotoxicity to both MCF-7/drug-sensitive and MCF-7/drug-resistant cells after second incubation. Moreover, results of confocal microscopy and flow cytometry of DOX-loaded micelles demonstrate the feasibility of this delivery system for effective therapy of drug-resistant tumours.

Keywords

Star-shaped co-polymer, multidrug resistance, micelles, doxorubicin, poly(ε-caprolactone), poly(ethyl ethylene phosphate)

1. Introduction

Biodegradable amphiphilic co-polymers have received significant interest in biomedical engineering such as in controlled drug delivery, sensing and image enhancement. Amphiphilic block co-polymers can self assemble to form nanosized polymeric micelles in an aqueous solution. The hydrophobic inner core can en-

* To whom correspondence should be addressed. Tel.: (886-3) 265-4550; Fax: (886-3) 265-4599; e-mail: mfhsieh@cycu.edu.tw

 DOI:10.1163/092050610X510533

capsulate hydrophobic drugs, while the hydrophilic outer shell provides the water-soluble property and stabilizes colloidal particles. Moreover, with a small particle size (<200 nm), polymeric micelles are a potential carrier for hydrophobic drugs owing to their ability to prolong residence time in blood circulation, enhance permeability and retention (EPR), reduce non-specific uptake by the reticuloendothelial system (RES) and overcome the recognition by P-glycoprotein [1–3]. However, micelles composed of linear amphiphilic co-polymer are unstable *in vivo* since dilution occurs in bloodstream and disassembly. On the other hand, micelles based on amphiphilic hyperbranched co-polymer have many advantages over that of linear polymeric micelles because of their highly functionalized globular architecture, low conformational freedom, a small hydrodynamic radius and increasing interstitial diffusion at the tumour site and good stability [4–6]. As a non-toxic, biodegradable, low viscosity and thermoplastic polyester, poly(ε-caprolactone) (PCL) is inexpensive and can be easily processed. PCL forms hydrophobic segments that have a short degradation time [7, 8]. Poly(ethylene glycol) (PEG), a water-soluble, non-immunogenic and non-toxic segment, is widely used in medical applications, but is known to oppose plasma protein adhesion [9]. However, PEG is a non-biodegradable polymer. Polyphosphoester polymer (PPE) is known as a biodegradable, biocompatible and water-soluble polymer, and is widely applied in biomedicine, such as in drug and gene delivery, as well as tissue engineering [10, 11].

Doxorubicin (DOX), an anthracycline drug, is commonly administered for treating breast cancer as well as ovarian, prostate, brain, cervix and lung cancer. However, DOX was found to have cardiac toxicity, a short half life-time and a low solubility in an aqueous solution [12, 13]. Related studies demonstrated that the multidrug resistance (MDR) is due to the P-glycoprotein (P-gp) efflux pump [1, 14, 15]. To prevent these phenomena, the DOX was encapsulated in the core of polymeric micelles by either chemical conjugation or physical entrapment [2, 16, 17].

To overcome the limitations of conventional micelles, this study attempts to synthesize the amphiphilic star-shaped co-polymer containing hydrophobic PCL and hydrophilic poly(ethyl ethylene phosphate) (PEEP). The star-shaped PCL macroinitiator is prepared by ring opening polymerization through use of a pentaerythritol ethoxylate initiator with the intention of obtaining the advantages of the water-soluble, non-toxic, biocompatible and non-immunogenic ethylene oxide segment. The structures of the star-shaped co-polymers are also characterized by proton nuclear magnetic resonance (^{1}H-NMR), gel-permeation chromatography (GPC) and Fourier transform infrared spectroscopy (FT-IR). Additionally, the self-assembled polymeric micelles are studied in an aqueous solution. An attempt has been made to elucidate the micellar formation, morphology and *in vitro* properties of such co-polymers for the DOX delivery applications. Moreover, the DOX-loaded nanoparticles composed of star-shaped co-polymers and DOX release profile are studied. Furthermore, the cell uptake and cytotoxic effect against human breast cancer cell lines (MCF-7/drug-sensitive and MCF-7/drug-resistant cell lines) are investigated.

2. Materials and Methods

2.1. Materials

Pentaerythritol ethoxylate (EO/OH: 15/4), ε-caprolactone, doxorubicin hydrochloride (DOX·HCl), 2-diphenyl-1,3,5-hexatriene (DPH), 2-chloro-2-oxo-1,3,2-dioxaphospholane and dimethylsulfoxide (DMSO) were purchased from Sigma-Aldrich. Stannous octoate ($Sn(Oct)_2$) was obtained from MP Biomedicals. Tetrahydrofuran (THF) was distilled from metallic sodium and benzophenone. Triethylamine (TEA), hexane and diethyl ether were purchased from Echo Chemicals.

For the cell-culture experiments, human breast cancer cell lines, drug-sensitive (MCF-7) and drug-resistant (MCF-7/adr) cell lines, were kindly donated by Dr. Y. H. Chen of School of Pharmacy, College of Medicine National Taiwan University, Taipei, Taiwan. 3-(4,5-Dimethylthiazol-2-yl)-2,5-diphenyl tetrazolium bromide (MTT) was obtained from Sigma-Aldrich. Dulbecco's Modified Eagle's Medium (DMEM) and antibiotic antimycotic were purchased from Invitrogen. The fetal bovine serum (FBS) was obtained from HyClone Thermo Fisher Scientific.

2.2. Synthesis of Star-Shaped Poly(ε-Caprolactone) Block Co-polymers

Figure 1 shows the synthesis procedures. The four-arm star-shaped PCL polymer was synthesized by ring-opening polymerization of ε-caprolactone in the presence of pentaerythritol ethoxylate as an initiator with $Sn(Oct)_2$ as a catalyst at 130°C for 6 h. A weighed amount of ε-caprolactone and pentaerythritol ethoxylate was then mixed in a round bottom flask under nitrogen, and 0.005% catalyst was added. Next, the reaction flask was placed in an oil bath under a mechanical stirrer at 130°C. Additionally, the product was dissolved in chloroform, and then precipitated three times in hexane/ether (1:9) and dried in vacuum.

2.3. Synthesis of Star-Shaped Poly(ε-Caprolactone)–Poly(Ethyl Ethylene Phosphate) Block Co-polymers

Ethyl ethylene phosphate (EEP) was synthesized by esterification of 2-chloro-2-oxo-1,3,2-dioxaphospholane with dry ethanol by a method described elsewhere [18]. A co-polymer of 4-arm star-shaped PCL and EEP was then prepared by ring-opening polymerization in THF at 35°C using $Sn(Oct)_2$ as catalyst [10]. Briefly, a mixture containing 4-arm star-shaped PCL, EEP monomer and $Sn(Oct)_2$ was dissolved in THF under nitrogen. Next, the reaction mixture was placed in a water bath at 35°C and stirred for 3 h. Thereafter, THF was removed, then precipitated in cold ether and dried under vacuum.

2.4. Characterization of Block Co-polymers

The formation of co-polymer was confirmed by ^{1}H-NMR, FT-IR and GPC. The FT-IR spectra were recorded on a FT-IR spectrometer (Jasco FT-IR 410) in the range of 4000 to 400 cm^{-1}. ^{1}H-NMR spectra of the block co-polymers were then recorded on a Bruker spectrometer operating at 500 MHz using $CDCl_3$ as solvent. Next, the

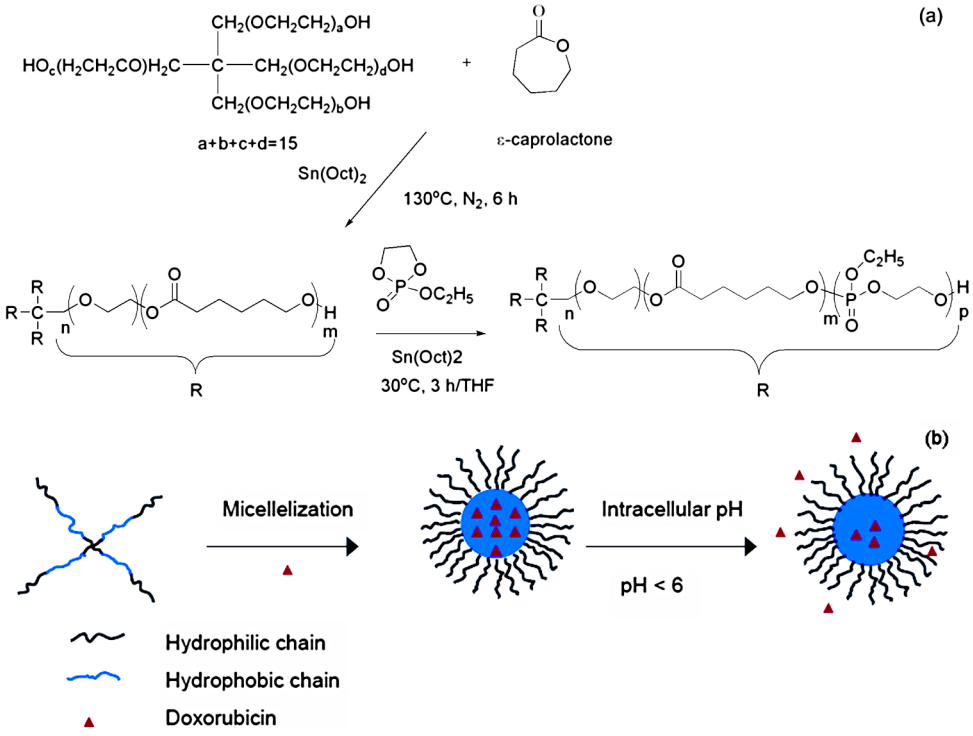

Figure 1. Synthesis of star-shaped co-polymer PCL–PEEP (a) and DOX-loaded PCL–PEEP micelles (b). This figure is published in colour in the online edition of this journal, that can be accessed *via* http://www.brill.nl/jbs

average molecular weight and polydispersity of the co-polymer were determined by GPC on a Viscotek GPCmax with VE 2001 RI detector using an AM GPC column. THF was used as eluent. The molecular weight was estimated using standard polystyrene samples.

2.5. Determination of Critical Micelle Concentration

The critical micelle concentration (CMC) of co-polymers was determined by UV-Vis spectroscopy (Jasco UV-530) using 1,2-diphenyl-1,3,5-hexatriene (DPH) as the fluorescent probe. Samples for UV-Vis measurement were prepared as described elsewhere [19]. The concentration of the aqueous co-polymer solution ranged between 0.01 and 10^{-6} mg/ml. Next, 2.0 ml polymeric solution was added to 20 µl DPH solution (0.4 mM in MeOH) to give a 4×10^{-6} M DPH/polymeric solution. The resulting solution was incubated in the dark for 5 h. Additionally, the UV-Vis absorption of incubated solution was measured in the range of 250–500 nm. Finally, the absorbance at 359 nm was selected to determine the CMC.

2.6. Preparation and Characterization of Micelles

For the DOX-unloaded micelles (placebo), the micellar solution was prepared by dissolving 20 mg co-polymer in 2.0 ml DMSO and then 10 ml deionized water (18.2 mΩ-cm purity) was added under stirring. The resulting solution was placed at room temperature for 3 h and, then, was transferred to a dialysis bag (MWCO 8000, Spectrum Laboratories) and dialyzed against deionized water for 24 h.

For the DOX-loaded micelles, 1.5 mg DOX was neutralized with an excess amount of TEA in 1.0 ml DMSO. The DOX solution was then added into the 2.0 ml DMSO solution of co-polymer (20 mg). These solutions were added to 2.0 ml deionized water under stirring for 3 h. The mixture was transferred for dialysis against deionized water for 12 h to produce DOX-loaded micelles. The water was replaced hourly for the first 3 h. The drug-loading efficiency (DLE) is defined as the weight percentage of DOX in micelles compared to the initial feeding amount of DOX. Next, the drug-loading content (DLC) is estimated from the mass of incorporated DOX divided by the weight of polymer. Additionally, the amount of DOX-loaded in micelles was determined by UV-Vis spectroscopy at 485 nm (Jasco UV-530) [20].

The particle size and particle size distribution were determined by dynamic light scattering (DLS) using a Zetasizer 3000HSA (Malvern) at a fixed angle of 90° and laser wavelength of 633.0 nm at 25°C. The micellar solutions were then prepared as above and diluted to 0.2 mg/ml before measurement. Next, the average diameter was estimated by the Conttin analytical method. Additionally, the zeta potential was measured using an aqueous dip cell in automatic mode using a Zetasizer 3000HSA.

2.7. In Vitro *DOX Release Study*

The experimental procedures are described elsewhere [21]. Briefly, 1.5 ml of DOX-loaded micellar solution was mixed in 0.5 ml PBS (0.1 M, pH 7.4) and acetate buffer solution (0.1 M, pH 5.4), and was transferred into a dialysis tube (MWCO 8000). The tube was immersed into a 15 ml buffer solution and was maintained at 37°C. At several time intervals, 1.0 ml buffer solution outside the dialysis bag was withdrawn for UV-Vis analysis at a wavelength of 485 nm and the entire medium was replaced with fresh buffer solution.

2.8. Measurement of Nitric Oxide (NO)

RAW 264.7 macrophage cells were seeded in a 24-well plate (1×10^5 cells/well) and incubated in 37°C, 5% CO_2 for 1 day. Micellar solution at various concentrations was added to the cells in a final volume of 0.8 ml. The supernatants were collected after 24 h and NO production was determined by Greiss reagent (1% sulfanilamide, 2.5% H_3PO_4, 0.1% naphthylethylenediamine dihydrochloride). Briefly, 100 µl culture medium was added to 100 µl Greiss reagent solution and incubated for 15 min. The absorbance was then measured at 540 nm. In the control experiment, macrophages were incubated in a lipopolysaccharide (LPS) solution

(10 ng/ml) and a micelle-free medium. Moreover, total protein extract was determined by Micro BCA Protein Assay.

2.9. *Haemolytic Test* in Vitro

The experimental procedure described here is an adjustment of standard F-756-00 [22], which is based on colorimetric detection of Drabkin's solution. Micellar solution at various concentrations (0.7 ml) was incubated in 0.1 ml rabbit red blood cells at 37°C and for 3 h. To ensure that fresh rabbit blood was used in the test, the haemoglobin in as-harvested plasma of rabbit blood was found to be less than 220 μg/ml, which is regarded as the basal level in the haemolysis test. Following incubation, the solution was centrifuged at 3800 rpm for 15 min. To determine the supernatant haemoglobin, 0.75 ml Drabkin's solution was added to 0.25 ml supernatant and the sample was allowed to stand for 15 min. The amount of cyanmethaemoglobin in the supernatant was measured using a spectrophotometer (Jasco UV-530) at a wavelength of 540 nm, and then compared to a standard curve (haemoglobin concentrations ranging from 0.003 to 1.2 mg/ml). The percent haemolysis refers to the haemoglobin concentration in the supernatant of a blood sample not treated with micelles to the obtained percentage of micelle-induced haemolysis. Finally, saline solution and double distilled water were used as negative and positive control, respectively.

2.10. In Vitro *Cytotoxicity Test*

MCF-7 and MCF-7/adr cells was seeded in a 96-well plate at a density of 1000 cells/well and incubated for 24 h before assay. Next, the cells were incubated in a medium containing various concentrations of DOX-loaded micelles or free DOX solution at 37°C under a humidified atmosphere containing 5% CO_2. Notably, the control for the micelle-treated experiment was a solution of media with placebo. For the free DOX experiment, the control was maintained in DOX-free media. The medium was replenished after 48 h with a fresh medium or a medium containing free DOX or DOX-loaded micelles and incubated for another 48 h. After 96 h, the MTT solution was added to each well, followed by 4 h of incubation at 37°C. The medium was subsequently removed and violet crystals were solubilised with DMSO. After shaking slowly twice for 5 s, the absorbance of each well was determined using a Multiskan Spectrum spectrophotometer (Thermo Electron) at 570 nm.

2.11. *Cellular Uptake of DOX*

For flow cytometry 1×10^5 cells (MCF-7 and MCF-7/adr) were incubated in the culture medium for 24 h and were treated with free DOX and DOX-loaded micelles, respectively (equivalent DOX concentration at 10 μg/ml). Cells in 12×75 Falcon tubes were placed on the FACSCalibur. The fluorescence intensity of DOX was collected at a 488 nm excitation and with a 575 nm band pass filter.

For confocal imaging the cells (MCF-7 and MCF-7/adr) were seeded in a MatTek glass bottom dish (1×10^5 cells/dish) and incubated for 24 h. The cells were

then incubated with free DOX and DOX-loaded micelles in a medium with DOX concentration at 10 μg/ml. After 24 h, the medium was removed and the cells were washed with cold PBS two times and fixed with 10% formalin solution. Finally, the cells were observed and imaged using confocal laser scanning microscopy (Fluo-View FV300, Olympus).

2.12. Statistical Analysis

All *in vitro* experiments were performed in triplicate or more unless otherwise stated. Values are presented as mean ± SD. Statistical significance of differences was tested using the unpaired Student's *t*-test. Statistical significance was determined at value of $P < 0.05$.

3. Results and Discussion

3.1. Synthesis and Characterization of Star-Shaped Poly(ε-Caprolactone)-Polyphosphoester Co-polymers

This initially involved preparing the macroinitiator. Four-arm star-shaped poly(ε-caprolactone) co-polymers were synthesized by ring-opening polymerization of ε-caprolactone and pentaerythritol ethoxylate as an initiator when using $Sn(Oct)_2$ as a catalyst (Fig. 1a). A previous study demonstrated the conversion of the initiator, pentaerythritol ethoxylate, to spirocyclic tin initiator [23]. In this study, pentaerythritol ethoxylate was used directly without conversion to the spirocyclic tin initiator. The star-shaped poly(ε-caprolactone) pre-polymers were prepared with different molecular weights in various molar ratios of ε-caprolactone and pentaerythritol ethoxylate ([CL]/[OH] = 50 and 100). According to ^{1}H-NMR, the peaks appearing at 3.39–3.63 ppm belonged to the methylene units of pentaerythritol ethoxylate; in addition, the signals at 4.05, 2.29, 1.64 and 1.32 ppm were assigned to the PCL arms. The number-average molecular weight of star-shaped PCL was based on ^{1}H-NMR ($M_n = (M_{w,int} + M_{w,CL}) \times DP_{CL} \times 4$) [24]. The star-shaped poly(ε-caprolactone)-polyphosphoesters were also synthesized by ring-opening polymerization of EEP and star-shaped poly(ε-caprolactone) polymer as the macroinitiator with $Sn(Oct)_2$ functioning as the catalyst (Fig. 1a). Typical signals of both methylene protons of ether chains and PCL in ^{1}H-NMR spectra were detected when using $CDCl_3$ as a solvent. Furthermore, the proton signals at 1.37 and 4.1–4.27 ppm are resonance signals of PEEP segments. The assignments resemble those in the literature [10].

The molecular weight and molecular weight distribution of star-shaped co-polymers were determined by GPC, in which THF was used as the eluent and monodisperse polystyrene as the standards. GPC results confirmed the formation of star-shaped co-polymers by increasing the molecular weight after ring-opening polymerization compared with macroinitiators. Table 1 summarizes the results.

Figure 2 shows the FT-IR spectra of star-shaped PCL and star-shaped PCL–PEEP co-polymers with various compositions of PCL segments. According to the FT-IR

spectra of star-shaped PCL, a large adsorption peak from the carbonyl group appears at 1730 cm^{-1}. In addition, the peak at 1180 cm^{-1} belongs to C–O stretching. In FT-IR spectra of star-shaped PCL–PEEP co-polymer reveals strong bands appearing at 1268 cm^{-1}, which are attributed to the P=O group of PEEP segments. Moreover, this band absorption increases when decreasing the molar ratios of PCL and PEEP. Furthermore, the P–O–C stretching bands appear at 1045 cm^{-1} and 968 cm^{-1}.

3.2. Preparation and Characterization of Micelles

The CMC values of PCL_{100}–$PEEP_{50}$ and PCL_{50}–$PEEP_{50}$ are 0.024 and 0.044 mg/ml, respectively. According to these results, not only does the co-polymer composition affect the CMC, but a lower CMC value was observed when the hydrophobic segment elongated. The star-shaped PCL–PEEP co-polymers can self

Table 1.
Properties of prepared star-shaped co-polymers

Sample	M_n of PCL macroinitiator[a]	M_n[b]	$M_{w,GPC}$	M_w/M_n	Yield (%)	CMC (mg/ml)	Ave size (nm)[c]	Polydispersity
PCL_{100}–$PEEP_{50}$	14 100	18 945	23 610	1.246	86	0.024	150.0	0.09
PCL_{50}–$PEEP_{50}$	7327	9105	11 066	1.215	75	0.044	133.9	0.12

[a] M_n based on feed ratio.
[b] M_n was calculated from ^{1}H-NMR.
[c] By dynamic light scattering at 25°C.

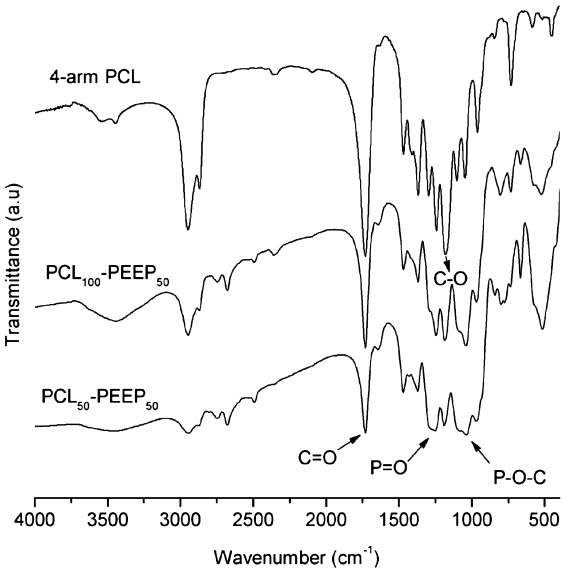

Figure 2. FT-IR spectra of star-shaped block co-polymers.

assemble to form nanosized micelles in an aqueous solution since the co-polymer consisted of the star-shaped hydrophobic PCL and hydrophilic EO and PEEP segments. The size and size distribution of co-polymeric micelle was evaluated by dynamic light scattering at 25°C (Table 1). The size distribution histogram of PCL_{100}–$PEEP_{50}$ displays the monomodal and narrow distribution (Fig. A1a). The average sizes of polymeric micelles are 150 and 133.9 nm for PCL_{100}–$PEEP_{50}$ and PCL_{50}–$PEEP_{50}$, respectively. This finding suggests that a larger hydrophobic state implies that more co-polymer chains aggregate into a micelle in order to minimize the interfacial energy, explaining the large size of the assembled micelles [25]. According to zeta potential measurements, the micelles were negatively charged in the range of −35.1 to −36.6 mV (Fig. A1b). This negative charge points towards a high electric charge on the surface of micelles, which may prevent the aggregation of micellar particles. The negative surface charge of star-shaped PCL–PEEP was significantly higher due to pentavalent phosphorus hetero-atoms of PEEP segments. This decrease in zeta potentials confirms that the presence of PEEP layer on the surface of micellar nanoparticles. The negative zeta potential of PEEP co-polymer has been described elsewhere [10, 26].

The size and morphology of micelles were evaluated further by observing the micelles using transmission electron microscopy (TEM). The TEM image of PCL_{100}–$PEEP_{50}$ micelles reveals a spherical shape (Fig. 3). The star-shaped co-polymers contained the hydrophobic segment, enabling the encapsulation of the hydrophobic drug in the core of micelles. Although a well-known anti-cancer reagent, DOX is limited by its sensitive toxicity of free drug to normal tissues, low water solubility of hydrophobic form and multidrug resistance effect. While attempting to

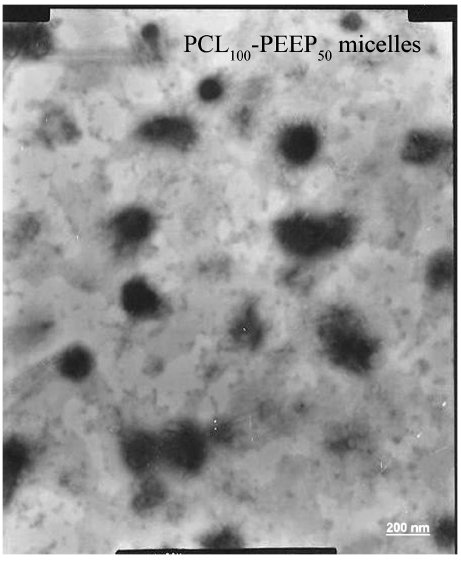

Figure 3. TEM image of PCL_{100}–$PEEP_{50}$ micelles.

overcome the toxicity of free drug and drug-resistance and increase the selectivity of the drug towards cancer cells, the hydrophobic DOX was physically entrapped in the core of micelles of star-shaped co-polymer. According to previous reports, the DLC increased with an increase in the molecular weight of the PCL segments [17, 20]. It could be attributed to the increase of hydrophobic segment of block co-polymers, the interaction between hydrophobic segment and hydrophobic drug was enhanced, leading to an increase in the DLC [21]. Therefore, in this study, PCL_{100}–$PEEP_{50}$ was selected for further studies in areas such as drug entrapment, safety and cytotoxicity evaluation and cellular uptake. The DOX-loaded micelle was of 156.1 nm particle size. A previous study found similar results, the size of DOX-loaded micelles increased slightly more than that of the DOX-free micelle [27]. As is well known, a polymeric micelle is an ideal nanocarrier for developing a drug-delivery system. Moreover, the particle size significantly affects *in vivo* performance. The particle sizes (<200 nm) may prevent a high level uptake of reticuloendothelial system (RES) and minimize renal excretion, as well as their ability to enhance permeability and preserve effects for passive tumour targeting [28, 29]. The drug loading efficiency and drug loading content were around 55.2 and 4.1%, respectively, when using a feed ratio of DOX to a co-polymer of 1.5:20.

3.3. Macrophage Response and Haemolysis of Polymeric Micelles

The toxicity of micelles toward macrophage cells was evaluated by the NO assay. Experimental results indicated that micelles did not affect NO production at concentrations of up to 0.25 mg/ml (Fig. 4). The NO production remained as low as that of the control group. Conversely, LPS (10 ng/ml) significantly increased the NO production of macrophage cells ($P < 0.01$). Compared with literature data, silica nanoparticles, regarded as relatively non-harmful to mammalian cells, at a concentration of 40 ppm increased 118.6% NO production in the treated group over that of the control group [30].

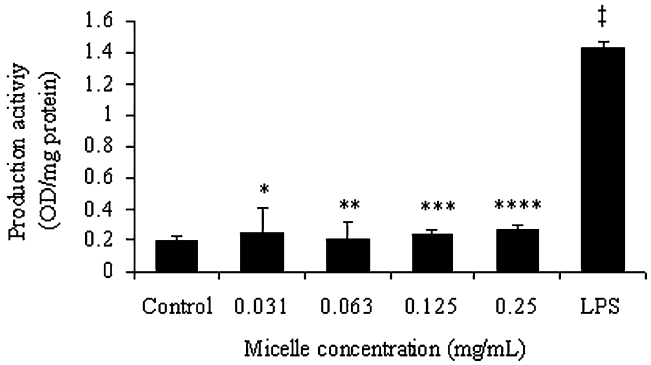

Figure 4. Effects of polymeric micelles on the levels of nitric oxide in RAW264.7 cells. Each bar represents the mean of four measurements ± SD. $^{*}P = 0.39$, $^{**}P = 0.9$, $^{***}P = 0.76$ and $^{****}P = 0.72$, not statistically different from control; $^{‡}P < 0.01$, significantly different from control.

Furthermore, the biocompatibility of polymeric micelles (placebo) with red blood cells (RBCs) was examined by performing a haemolysis test. According to Fig. 5, an increase in the micellar concentration slightly increased the haemolysis percentage of RBCs. RBCs when contacting with 2 mg/ml polymeric micelles caused a slight haemolysis comparing with that of the negative control (saline solution) and was similar to the blank solution (PBS buffer). In conjunction with the macrophage response, the haemolysis test suggested that the star-shaped polymeric micelle prepared in this study had a moderate toxicity and was safe for intravenous injection.

3.4. In Vitro *Release of DOX from Polymeric Micelles*

Figure 6 displays the *in vitro* release profiles of DOX from the polymeric micelles (PCL_{100}–$PEEP_{50}$) in PBS (0.1 M, pH 7.4) and acetate buffer solutions (0.1 M, pH 5.4) at 37°C. Experimental results indicated an initial burst release of DOX, followed by a sustained release for about 72 h. The initial burst release of DOX from micelles could be attributed to the diffusion of DOX located in close proximity to the surface of particles or within the hydrophilic shell [31]. The total release of DOX in a period of 96 h with pH 7.4 and 5.4 was 38% and 57% of the total DOX concentration, respectively. However, the release of DOX at a pH value of 5.4 was found to be faster than that at a pH value of 7.4. A similar pattern was observed in the acidic condition previously [17, 32]. Above results could be attributed to the re-protonation of the amino group of DOX and the faster degradation of the micelle core at lower pH values. This pH-dependent release profile is of particular interest. As is expected, the greater portion of DOX-loaded micelles remains in the micelles cores for a certain period of time in plasma after intravenous administration. Moreover, these micelles have the potential for a prolonged DOX retention time in the

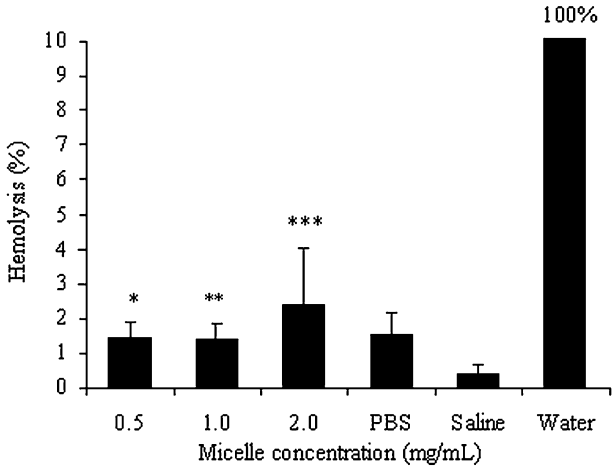

Figure 5. Hemolytic test on polymeric micelles. Each bar represents the mean of three measurements ±SD. * $P = 0.69$, ** $P = 0.33$ and *** $P = 0.29$, not statistically different from PBS solution.

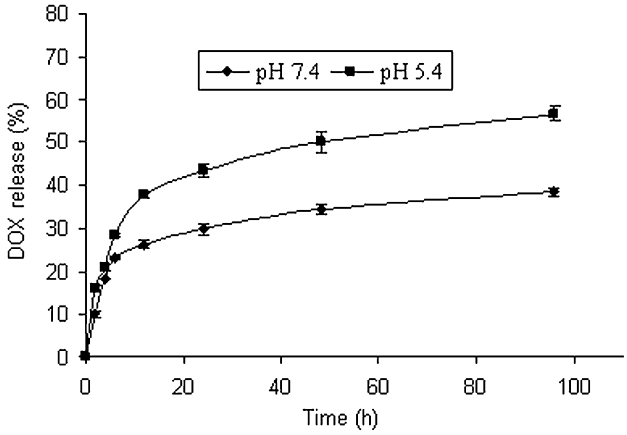

Figure 6. Effect of pH on DOX release profiles from DOX-loaded micelles at 37°C.

blood circulation. However, a faster release may occur at a low local pH surrounding the tumour site or by the more acidic environment inside the endosome and lysosome of tumour cells after cellular uptake of micelles through endocytosis.

3.5. In Vitro *Cytotoxicity of DOX-Loaded Micelles*

The *in vitro* cytotoxic effects of DOX-loaded star-shaped co-polymer based micelles and free DOX were studied using a tetrazolium dye (MTT assay) in human breast cancer cell lines MCF-7 and MCF-7/adr. The cell viability was determined against various equivalent concentrations of DOX ranging from 0.01 to 20 μg/ml. The medium was replenished after 48 h with fresh medium or a medium containing free DOX or DOX-loaded micelles, and incubated for another 48 h during the 96-h viability test. Notably, both the single dose and multiple injections are used in preclinical and clinical studies. The second dose was added during *in vitro* test in order to evaluate the efficacy of DOX-loaded micelles in multiple doses mode. It is possible that IC_{50} of triple incubations will decrease in comparison with double incubations. Due to the increase of DOX concentration and time incubation will decrease the cell viability. Furthermore, a combinatory formulation may be used rather than increasing dosage or multiple dosing. For example, using a chemosensitizer can reverse multidrug resistance to, e.g., chlorpromazine and verapamil caused by overexpression of P-gp in cancer cells [33, 34]. Figure 7 shows the cell viability when treated twice with DOX-loaded micelles and free DOX toward drug-sensitive and drug-resistant cell lines. The cell viability significantly decreased with increasing DOX concentration when the cells were incubated once or twice with free DOX or DOX-loaded micelles in culture medium. Table 2 lists the half-lethal dose (IC_{50}) of free DOX and DOX-loaded micelles for both MCF-7 and MCF-7/adr cells. It can be seen that the higher the drug concentration, the lower the cell viability. The cytotoxicity of free DOX against MCF-7 cells ($IC_{50} = 0.032$) was greater than the DOX-loaded micelles ($IC_{50} = 0.41$) ($P < 0.05$, unpaired Student's t-test). Recent

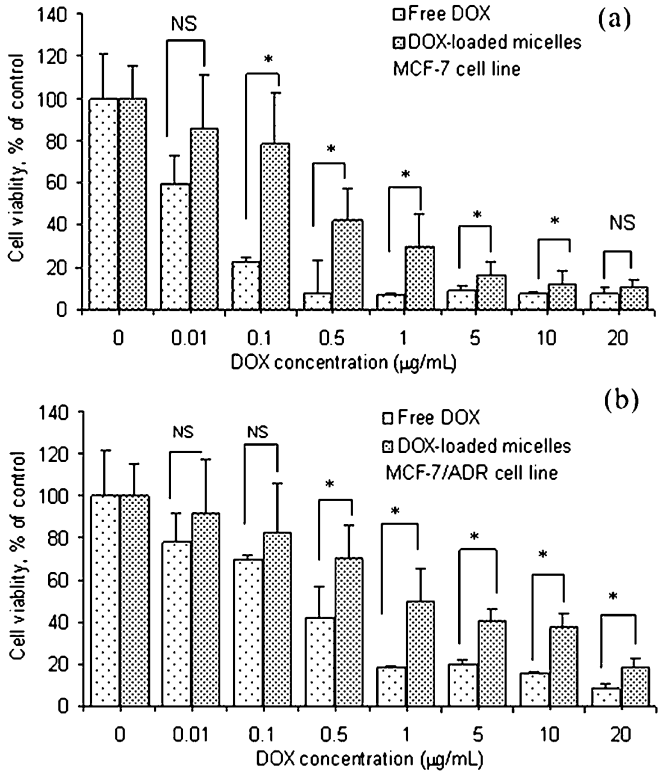

Figure 7. Cytotoxicity of MCF-7 cells (a) and MCF-7/adr cells (b). The cells were incubated with free DOX and DOX-loaded micelles for 96 h at 37°C. Each bar represents the mean of four measurements ± SD. * $P < 0.05$, significantly different between cells treated with free DOX and DOX-loaded micelles; NS, not significant ($P > 0.05$).

Table 2.
IC_{50} values of free Dox and Dox-loaded micelles for MCF-7 and MCF-7/adr cells

	MCF-7		MCF-7/adr	
Free DOX	0.46[a]	0.032[b]	0.65[a]	0.39[b]
DOX-loaded micelles	10.1[a]	0.41[b]	6.71[a]	1.45[b]

[a] Cell was incubated once with DOX-containing medium.
[b] Cell was incubated twice with DOX-containing medium.

reports demonstrated that free DOX had a higher cytotoxicity than DOX nanoparticles when nanoparticles accumulate into the tumour cells through passive targeting endocytosis (a process in which nanoparticles internalize into the cells by the enhanced permeability and retention effect) [21, 32, 35, 36]. As compared with a recent report, DOX conjugated stearic acid-*g*-chitosan oligosaccharide polymeric

micelles showed a lower IC_{50} value than free DOX (4.54 *versus* 0.11). Conversely, free DOX showed a lower cytotoxicity than DOX nanoparticles when nanoparticles can be internalized by the tumour cells *via* receptor-mediated endocytosis such as folate (a process in which nanoparticles internalize into the cells by first binding to specific receptors on the cell surface before being invaginated) [32, 37, 38]. In this study, DOX-loaded micelle exhibited a lower cytotoxicity than free DOX because free DOX could easily diffuse into the cells as compared to DOX encapsulated in micelles. DOX-loaded micelles were internalized into the tumour cells through passive targeting endocytosis; in addition, DOX was released slowly and incompletely from the micelles [39]. However, the cytotoxicity of DOX-loaded micelles was equivalent to that of free DOX in MCF-7 cells when the concentration exceeded 10 μg/ml (Fig. 7a). Additionally, the IC_{50} value of DOX-loaded micelles decreased 4.6-fold in comparison with 1.6-fold of free DOX for drug-resistant cells (Fig. 7b). More promising results were obtained from drug-sensitive cells. The IC_{50} value decreased 25-fold for DOX-loaded micelles compared with 14-fold for free DOX when the MCF-7 cells were incubated with second dose of a medium containing DOX. This finding suggests that DOX-loaded micelles have higher potential anti-tumour activity than that of free DOX in both cell lines. These results correlated with the results of flow cytometry, in which the DOX-loaded micelles exhibited a similar cellular uptake of free DOX in drug-sensitive cells and a higher cellular uptake of free DOX in drug-resistant cells (Fig. 8). This observation could be attributed to the internalization of nanoparticles by endocytosis. The nanoparticles are hypothesized to escape the endo-lysosomal pathway and the anionic charge of nanoparticle surface changes to cationic in the acidic pH of secondary endosomes/lysosomes [34]. Thereafter, DOX was released from encapsulated nanoparticles into the cellular cytoplasm, which can prevent tumour cells from effluxing the DOX due to the expression of P-gp [40]. A placebo was also treated with MCF-7 cells to evaluate the cytotoxicities of materials. Notably, the placebo was found to be non-toxic to the cells at a concentration up to 0.5 mg/ml (data not shown).

3.6. Cellular Uptake of DOX-Loaded Micelles

The cellular uptake behaviour of DOX-loaded micelles in both drug-sensitive and drug-resistant cells was obtained from flow cytometry. Figure 8 shows the histogram of cellular uptake activities of drug-sensitive and drug-resistant cells incubated with free DOX and DOX-loaded micelles. The culture medium without any DOX content was used as the control and displayed only the auto-fluorescence of the cells. The drug-sensitive cells incubated with DOX-loaded micelles exhibited a similar fluorescence intensity in comparison with that of free DOX (Fig. 8a). However, when the DOX-loaded micelles were treated with drug-resistant cells, its fluorescence intensity was 4–6-times higher than that of free DOX (Fig. 8b). Free DOX was blocked for entry into the cells due to the high expression of P-glycoprotein on the drug-resistant cell surface [40]. The flow cytometry results suggested that

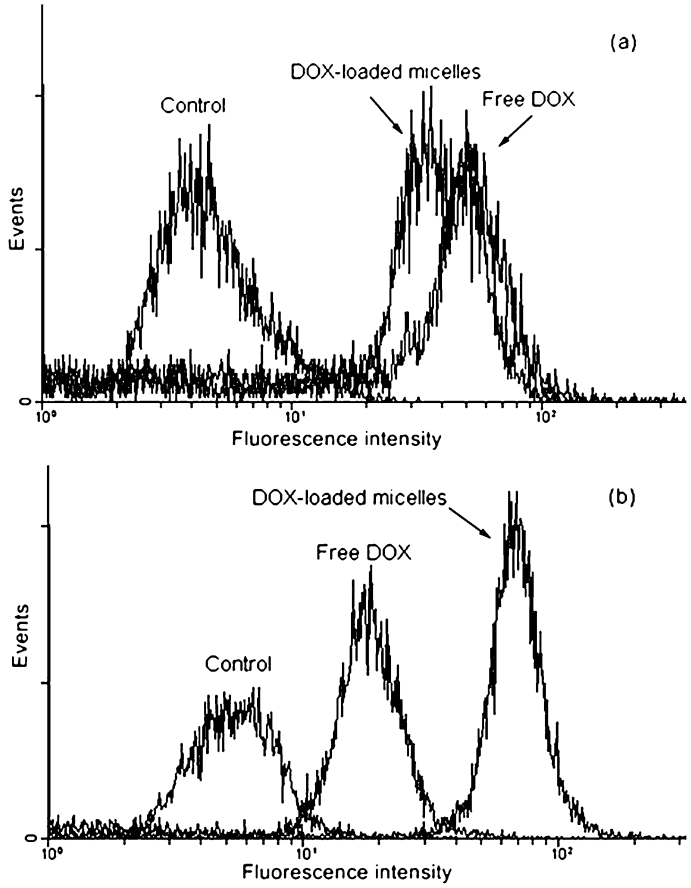

Figure 8. Flow cytometry histogram profile of MCF-7 cells (a) and MCF-7/adr cells (b) that were incubated with free DOX and DOX-loaded micelles (DOX concentration 10 μg/ml) for 24 h at 37°C.

encapsulation of DOX may be able to prevent P-glycoprotein-mediated multidrug resistance. The drug escaped from the endosomes/lysosomes and was found only on cytoplasm making cytotoxicity of micelle-mediated uptake of DOX was lower than that of free DOX (Figs 7 and 9). This is also confirmed the sustained release of DOX from micelles in this study. These data suggest that DOX-loaded micelles are a promising means of treating multidrug resistant tumours.

The extent of cellular uptake and internalization of DOX-loaded micelles into drug-sensitive and drug-resistant cells were observed by confocal microscopy. According to Fig. 9, after 24 h of incubation with DOX-loaded micelles, a strong DOX fluorescence was observed in the cytoplasm, as well as a weak fluorescence in nuclei of cells. The signal appearing in nuclei was attributed to the DOX molecule release from the micelles, demonstrating the controlled and sustained release of drugs from polymeric micelles. The fluorescence in cytoplasm indicated that the DOX-loaded micelles were internalized by cells through endocytosis. The acidic

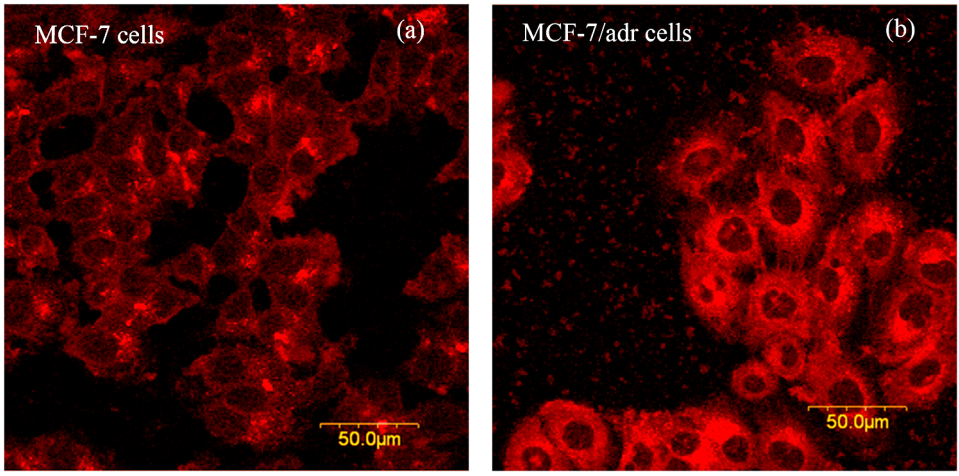

Figure 9. Confocal images of MCF-7 (a) and MCF-7/adr (b) cells after incubation with DOX-loaded micelles at the equivalent 10 μg/ml DOX concentration (scale bar = 50 μm). This figure is published in colour in the online edition of this journal, that can be accessed *via* http://www.brill.nl/jbs

endosomal compartment (pH 5.5–5.0) caused the release of DOX into the cytoplasm [41]. However, after incubation with free DOX, the DOX fluorescence was observed in nuclei of cell instead of cytoplasm (data not shown). This is reasonable since DOX is a small molecule and could transport freely through both the plasma membrane and nuclear membrane *via* a passive pathway of diffusion. Similar results were also observed previously with 4T1 cells [32] and human breast cancer cells (MCF-7) [21]. DOX is widely known as DNA intercalation and topoisomerase II inhibitor for cancer chemotherapy, all of which require DOX accumulation in the nuclei. Therefore DOX encapsulated nanoparticles may lead to a lower cytotoxicity than that of free DOX (Fig. 7). However, *in vivo* application using DOX encapsulated nanoparticles were shown to increase circulation time, decrease side effect and improve drug bioavailability [40]. Additionally, Fig. 9b, obtained from drug-resistant cells, shows that DOX-loaded mielles presented higher intracellular DOX uptake than drug-sensitive cells (Fig. 9a). This could be attributed to the prevention of multidrug resistance. The results suggest that present micelles may able to circumvent P-glycoprotein-mediated multidrug resistance, and then avoid recognition by the P-glycoprotein efflux pump, leading to high intracellular drug concentration.

4. Conclusion

This study has synthesized a series of star-shaped poly(ε-caprolactone)-polyphosphoester co-polymers by using ethoxylated pentaerythritol initiator as potential doxorubicin delivery system. The co-polymer structures were confirmed by ^{1}H-NMR, FT-IR and GPC. The co-polymers formed nanosized micellar structures in an aqueous solution of 133.9 and 150 nm for PCL_{50}–$PEEP_{50}$ and PCL_{100}–$PEEP_{50}$, respectively. Additionally, the *in vitro* drug-release profiles from the mi-

celles were pH dependent. The DOX release from micelles at pH 5.4 was faster than that at pH 7.4. Safety evaluation of polymeric micelles *in vitro* revealed a low toxic star-shaped co-polymeric micelle. Furthermore, results of this study with respect to the cytotoxicity, flow cytometry and confocal microscopy observations of DOX-loaded micelles demonstrate the feasibility of this system for treatment of drug-sensitive cancer as well as drug-resistant cells.

Acknowledgements

The authors would like to thank the National Science Council of the Republic of China, Taiwan under Contract No. NSC97-2218-E-033-001 and NSC 98-2221-E-033-072 and the project of the specific research fields in the Chung Yuan Christian University under grant CYCU-97-CR-BE for financially supporting this research. Ted Knoy is appreciated for his editorial assistance.

References

1. A. K. Sharma, L. Zhang, S. Li, D. L. Kelly, V. Y. Alakhov, E. V. Batrakova and A. V. Kabanov, *J. Control. Rel.* **131**, 220 (2008).
2. G. Kwon, S. Suwa, M. Yokoyama, T. Okano, Y. Sakurai and K. Kataoka, *J. Control. Rel.* **29**, 17 (1994).
3. G. S. Kwon and T. Okano, *Adv. Drug Deliv. Rev.* **21**, 107 (1996).
4. S. Chen, X. Z. Zhang, S. X. Cheng, R. X. Zhuo and Z. W. Gu, *Biomacromolecules* **9**, 2578 (2008).
5. K. Kono, C. Kojima, N. Hayashi, E. Nishisaka, K. Kiura, S. Watarai and A. Harada, *Biomaterials* **29**, 1664 (2008).
6. F. Wang, T. K. Bronich, A. V. Kabanov, R. D. Rauh and J. Roovers, *Bioconjug. Chem.* **19**, 1423 (2008).
7. J. Panyam and V. Labhasetwar, *Adv. Drug Deliv. Rev.* **55**, 329 (2003).
8. C. Shen, S. Guo and C. Lu, *Polym. Degrad. Stabil.* **92**, 1891 (2007).
9. H. Otsuka, Y. Nagasaki and K. Kataoka, *Adv. Drug Deliv. Rev.* **55**, 403 (2003).
10. Y. C. Wang, L. Y. Tang, T. M. Sun, C. H. Li, M. H. Xiong and J. Wang, *Biomacromolecules* **9**, 388 (2008).
11. Z. Zhao, J. Wang, H. Q. Mao and K. W. Leong, *Adv. Drug Deliv. Rev.* **55**, 483 (2003).
12. T. Maria and H. Clifford, *Cancer* **100**, 2052 (2004).
13. J. Cui, C. Li, W. Guo, Y. Li, C. Wang, L. Zhang, L. Zhang, Y. Hao and Y. Wang, *J. Control. Rel.* **118**, 204 (2007).
14. R. Krishna and L. D. Mayer, *Eur. J. Pharm. Sci.* **11**, 265 (2000).
15. N. Marchi, K. Hallene, K. Kight, L. Cucullo, G. Moddel, W. Bingaman, G. Dini, A. Vezzani and D. Janigro, *BMC Med.* **2**, 37 (2004).
16. N. Cao and S. S. Feng, *Biomaterials* **29**, 3856 (2008).
17. M. F. Hsieh, N. V. Cuong, C. H. Chen, Y. T. Chen and J. M. Yeh, *J. Nanosci. Nanotechnol.* **8**, 2362 (2008).
18. J. Wen, G. J. A. Kim and K. W. Leong, *J. Control. Rel.* **92**, 39 (2003).
19. C. Lu, S. Guo, L. Liu, Y. Zhang, Z. Li and J. Gu, *J. Polym. Sci. Polym. Phys.* **44**, 3406 (2006).
20. H. M. Aliabadi, A. Mahmud, A. D. Sharifabadi and A. Lavasanifar, *J. Control. Rel.* **104**, 301 (2005).
21. X. Shuai, H. Ai, N. Nasongkla, S. Kim and J. Gao, *J. Control. Rel.* **98**, 415 (2004).

22. *Standard Practice for Assessment of Hemolytic Properties of Materials*. ASTM International, West Conshohocken, PA (2000).
23. A. Finne and A.-C. Albertsson, *Biomacromolecules* **3**, 684 (2002).
24. J. Choi, I. K. Kim and S. Y. Kwak, *Polymer* **46**, 9725 (2005).
25. J. Zhang, L. Q. Wang, H. Wang and K. Tu, *Biomacromolecules* **7**, 2492 (2006).
26. J. Cheng, J. X. Ding, Y. C. Wang and J. Wang, *Polymer* **49**, 4784 (2008).
27. Y. Zhang and R. X. Zhuo, *Biomaterials* **26**, 6736 (2005).
28. K. E. Schmalenberg, L. Frauchiger, L. Nikkhouy-Albers and K. E. Uhrich, *Biomacromolecules* **2**, 851 (2001).
29. C. L. Peng, M. J. Shieh, M. H. Tsai, C. C. Chang and P. S. Lai, *Biomaterials* **29**, 3599 (2008).
30. E. J. Park and K. Park, *Toxicol. Lett.* **184**, 18 (2009).
31. C. Allen, D. Maysinger and A. Eisenberg, *Colloids Surfaces B: Biointerfaces* **16**, 3 (1999).
32. M. Prabaharan, J. J. Grailer, S. Pilla, D. A. Steeber and S. Gong, *Biomaterials* **30**, 3009 (2009).
33. C. W. Yde, M. P. Clausen, M. V. Bennetzen, A. E. Lykkesfeldt, O. G. Mouritsen and B. Guerra, *Anti-Cancer Drugs* **20**, 723 (2009).
34. M. D. Chavanpatil, Y. Patil and J. Panyam, *Int. J. Pharm.* **320**, 150 (2006).
35. C. Chun, S. M. Lee, C. W. Kim, K. Y. Hong, S. Y. Kim, H. K. Yang and S. C. Song, *Biomaterials* **30**, 4752 (2009).
36. F. Q. Hu, L. N. Liu, Y. Z. Du and H. Yuan, *Biomaterials* **30**, 6955 (2009).
37. S. Q. Liu, N. Wiradharma, S. J. Gao, Y. W. Tong and Y. Y. Yang, *Biomaterials* **28**, 1423 (2007).
38. Z. Zhang, S. Huey Lee and S. S. Feng, *Biomaterials* **28**, 1889 (2007).
39. C. L. Lo, S. J. Lin, H. C. Tsai, W. H. Chan, C. H. Tsai, C. H. D. Cheng and G. H. Hsiue, *Biomaterials* **30**, 3961 (2009).
40. Y. Yi, J. H. Kim, H.-W. Kang, H. S. Oh, S. W. Kim and M. H. Seo, *Pharm. Res.* **22**, 200 (2005).
41. H. Zhao and L. Y. L. Yung, *Int. J. Pharm.* **349**, 256 (2008).

Appendix A

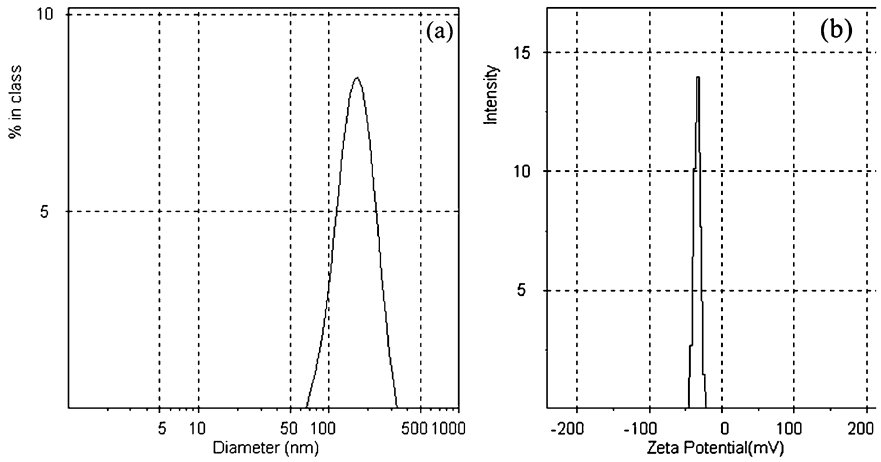

Figure A1. (a) The size distribution histogram of PCL_{100}–$PEEP_{50}$ micelles. (b) Zeta potential of PCL_{100}–$PEEP_{50}$ micelles.